JOURNAL OF MATERIALS SCIENCE 26 (1991) 6237–6243

Comparison of methods for crack tip opening displacement toughness determination

R. K. PANDEY, A. N. KUMAR, P. SUNDARAM
Centre for Materials Science and Technology, Indian Institute of Technology, Delhi, Hauz Khas, New Delhi-110016, India

The crack tip opening displacement (CTOD) initiation toughness has been obtained by different methods in Cr and Cr–Mo steels at 30, 200 and 400 °C. The crack tip stretching and grain deformation has been investigated by scanning electron microscope and optical microscopic studies and by microhardness measurements. The resistance curve approach is used employing the average and the maximum crack growth and the initiation toughness determined are with respect to 0.2 mm crack growth ($\delta^{0.2}$), the stretched zone width (SZW) and also using a blunting line approach. In addition, an initiation toughness using stretched zone depth (SZD) measurement is also obtained. The various initiation toughness values have been compared and an attempt has been made to identify the realistic plane strain CTOD toughness amongst the different values. The $\mathcal{J}$–CTOD relationship has also been investigated.

1. Introduction

The crack tip opening displacement (CTOD) is used as the elastic–plastic toughness parameter and hence also for providing inspection standard to structures where fracture or failure is preceded by ductile crack growth. The standard for CTOD (δ) measurement is provided by BS 5762 [1] using a clip gauge method in bending geometry. The method involves use of rotation factor (r) to convert the crack mouth opening displacement (CMOD) into the CTOD. The rotation factor is standardized only for the three-point bend geometry and some empirical approaches have to be used to determine the rotation factor for other geometries [2, 3]. In addition, the rotation factor changes with a change in the ratio of plastic to elastic component of displacement as well as with the stable crack growth [4, 5]. Contradictory reports have been made by various investigators with regard to the numerical value of rotational factor in different geometries and the method used for its evaluation. Pratap and Pandey have even suggested a method to evaluate CTOD without the use of the rotational factor [6]. Kolednik, recently [7] suggested a value of $r = 0.96$ in place of 0.4 as recommended by BS 5762 leading to a further uncertainty.

Besides the rotation factor, another point of controversy is the definition of the crack initiation CTOD. The latter may be defined by various ways e.g. (a) CTOD corresponding to nil physical crack growth, (b) CTOD corresponding to point of intersection of δ resistance curve with the blunting line analogus to J toughness determination [8]. (c) CTOD corresponding to a specified amount of crack growth (2%, 0.2 mm etc.) on the δ-R curve and (d) CTOD at the critical stretched zone width (SZW). The ASTM Committee on Fracture testing [9] has also in fact suggested finding the initiation CTOD for the 0.2 mm crack growth on δ–R curve. The European Group on Fractures (EGF) [10] has on the other hand, proposed a different methodology to evaluate the initiation toughness, CTOD.

In view of the prevailing multiplicity of opinions with regard to the crack initiation toughness in ductile alloys, the present investigation has been undertaken. A considerable difference may be expected between the initiation toughness (δ_i) values obtained by different approaches leading to an unrealistically conservative value on one hand and a too optimistic value on the other hand. The different methods for δ_i evaluation hence need to be compared and the values of δ_i need to be checked against a more direct method based on the microscopic measurements near the crack tip. The present investigation has been conducted with the above objectives in mind.

2. Experimental procedure

2.1. Materials and test specimens

The investigation was carried out using two structural low alloy steels, i.e. a $2\frac{1}{4}$ Cr–1 Mo steel and a $\frac{1}{2}$ Mo steel. The chemical composition and tensile properties of the alloys are shown in Table I.

The single-edge notched (SEN) bend specimens were machined as per ASTM standard with thickness, $B = 11$ mm, width, $W = 22$ mm and crack depth to width ratio, $a/W = 0.5$. Fatigue precracking was provided using standard method [1].

2.2. Fracture mechanics test

The specimens were tested on an Instron machine of 5 tonne capacity under a three-point bend loading. The

TABLE I Chemical composition (wt %) and tensile properties of alloys

Alloy	C	Mn	Si	S	P	Cr	Mo
Mo steel	0.21	0.81	0.255	0.023	0.034	0.22	0.45
Cr–Mo steel	0.14	0.48	0.330	0.026	0.035	2.07	0.86

Alloy	Testing temperature (°C)	Yield strength σ_y (MPa)	Tensile strength σ_u (MPa)	Elongation (%)	RA (%)	Strain hardening exponent, n
	30	349	540	33	68	0.190
Mo steel	200	294	532	25	60	0.212
	400	306	579	28	56	0.203
	30	389	566	33	78	0.170
Cr–Mo steel	200	337	503	30	79	0.203
	400	331	515	26	76	0.186

CMOD was measured using a clip gauge and output was taken on a d.c. microvoltmeter. The load point displacement (LPD) was measured with a dial gauge. The CMOD and LPD readings were taken at regular intervals with load. The tests were conducted at ambient temperatures (30 °C), 200 and 400 °C. For other than ambient temperature tests, two heating pads consisting of heating coils of 200Ω resistance were placed on either sides of the specimen. Electrical insulation was provided by using mica sheets between the heating pad and the specimen surface. Current was passed through the heating coil by regulated power supply and the temperature was measured by a thermocouple spot welded near the crack.

The loading was continued to an appropriate level in the elastic–plastic region to allow some crack growth in the specimen. Four to six identical specimens were loaded to give varying amounts of crack growth. The actual amount of crack growth was measured after break opening the specimen in liquid nitrogen. The average crack growth (Δa_{av}) using the nine-point average method and the mid thickness (maximum) crack growth (Δa_{max}) were measured on the broken surfaces.

2.3. Microscopic studies of stretched-region

For studying the profile of stretched zone (SZ) specimens were sectioned at the mid thickness. The surface was polished and mounted vertically so that the mid thickness plane comes under the SEM beam (Fig. 1). The back tilt was varied between 10 and 30° to make the profile clear. The stretched zone width (SZW) as well as the depth (SZD) were measured. The details are reported elsewhere [11].

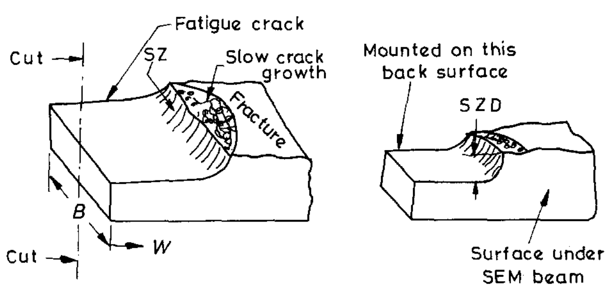

Figure 1 Schematic diagram of SZD measurement *B* thickness, *W* width of specimen.

The transverse section of the fracture in the vicinity of stretched zone was investigated using an optical microscope to reveal grain deformation and structural features. The microhardness measurements were also taken across the SZ on the transverse section to ascertain grain deformation characteristics.

3. Results

3.1. Determination of CTOD and CTOD-resistance (δ–*R*) curves

To obtain the CTOD at the original crack tip, the change in rotation centre due to physical crack growth was taken into account resulting in an expression for CTOD [11]

$$\delta = \delta_e + \delta_p = \frac{K^2(1-\nu^2)}{2\sigma_y E} + V_{gp}\left(\frac{a + \Delta a + z + r(W-a-\Delta a)}{r(W-a-\Delta a)}\right)^{-1} \quad (1)$$

where δ_e and δ_p are the elastic and plastic components of CTOD, K the stress intensity factor corresponding to the critical load, σ_y, E and ν the yield strength, elastic modulus and Poisson's ratio, respectively, V_{gp} the plastic component of CMOD and r the rotation factor. A value of $r = 0.4$ was used along the line of BS 5762 recommendations. The values of δ were computed at different amount of crack growth by substituting the average as well as the maximum crack growth separately in the above equation and termed as δ_{av} and δ_{max}, respectively. It was noted that the proposed BS 5762 method to find CTOD (without considering a change in rotation centre) resulted in a much more conservative value and was hence discarded in favour of Equation 1.

In attempting to draw δ–*R* curves, it was noticed that the best fit curves were either linear or non-linear with second-degree polynomial. This is contrary to the recommendations by BS 5762 or ASTM E 813–88 where a linear regression line is suggested for the best fit for the δ–*R* and *J*–*R* curves respectively. All the *R* curves were analysed by using both the linear and the non-linear regression analysis and the best fit was used

TABLE II Best fit equations for δ–*R* curves (δ in μm, Δa in mm)

Alloy	Test temperature (°C)	δ_{av} against Δa_{av}	δ_{max} against Δa_{max}
		δ_{av} =	δ_{max} =
	30	$289 + 173\Delta a + 77\Delta a^2$	$319 + 4.6\Delta a + 86\Delta a^2$
Mo steel	200	$228 + 33.3\Delta a + 84.5\Delta a^2$	$49 - 35.7\Delta a + 59.6\Delta a^2$
	400	$82 + 419\Delta a + 11.9\Delta a^2$	$96 + 202\Delta a + 19.5\Delta a^2$
	30	$158 + 834.3\Delta a$	$75 + 579\Delta a$
Cr–Mo steel	200	$285 + 696.5\Delta a$	$151 + 555.7\Delta a$
	400	$237 + 414.1\Delta a$	$191 + 287\Delta a$

TABLE III Description of crack tip stretched zone

Alloy	Test temperature (°C)	SZW (μm)	SZD (μm)	Blunting angle, θ (deg)	*d* (μm)	Degree of straining VHN
Mo Steel	30	170	137	39	360	35
	200	130	115	41	280	24
	400	100	55	29	230	19
HAZ	30	129	121	43	—	—
Cr–Mo steel	30	110	58	28	333	46
	200	140	101	36	392	52
	400	170	111	33	450	59
HAZ	30	91	69	37	—	—

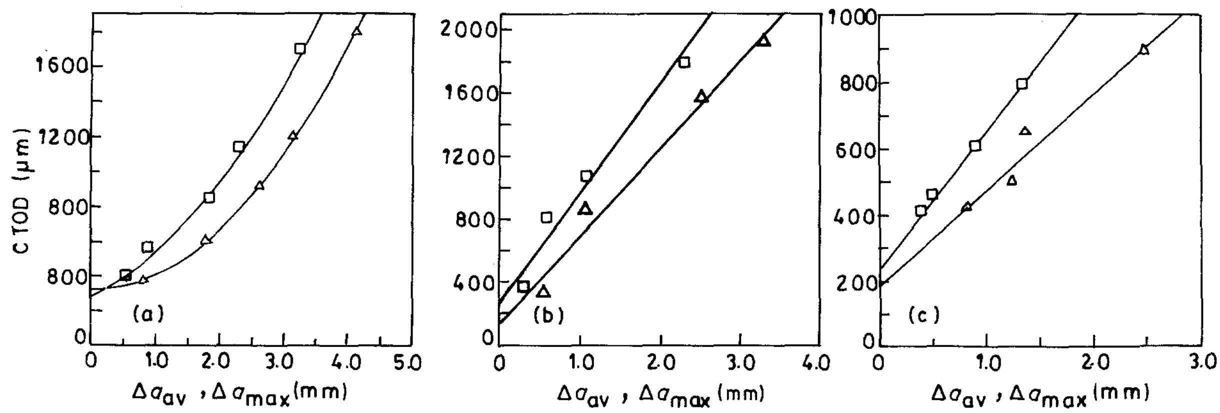

Figure 2 Typical δ-resistance curves (a) Mo steel, 30 °C (b) Cr–Mo steel, 200 °C (c) Cr–Mo steel, 400 °C (□ $\delta_{av} - \Delta a_{av}$, △ $\delta_{max} - \Delta a_{max}$).

as the representative *R* curve. The *R* curves were obtained using the average as well as the maximum crack growth, δ_{av} against Δa_{av}, and δ_{max} against Δa_{max}. Typical *R* curves are presented in Fig. 2. The best fit equations for δ–*R* curves are reported in Table II.

3.2. Stretched zone studies

The stretched zone width, stretched zone depth and blunting angle θ (calculated as $\tan^{-1}$ (SZD/SZW) results are given in Table III. Table III also includes some data on stretched zone measurements taken from the heat affected zone (HAZ) of the alloys the details of which are reported elsewhere [11]. It is seen from Table III that the blunting angle varies between 28 and 43° and is thus smaller than the conventionally assumed angle of 45°.

The microscopic study of the transverse section of the fracture surface from the stretched region revealed an elongated grain structure (Fig. 3). The length of the deformed region, *d*, consisting of elongated ferrite grains was measured along the crack propagation direction and reported in Table III. The length, *d*, is found to decrease with increasing temperature for the

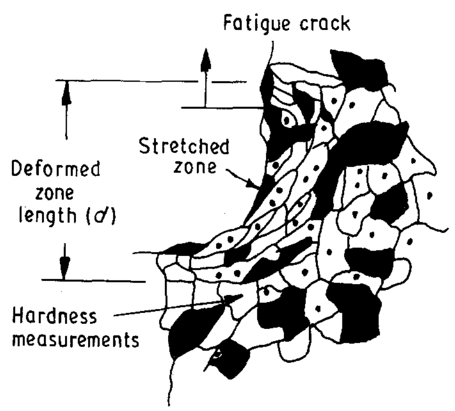

Figure 3 Schematic representation of elongated grain structure near stretched zone.

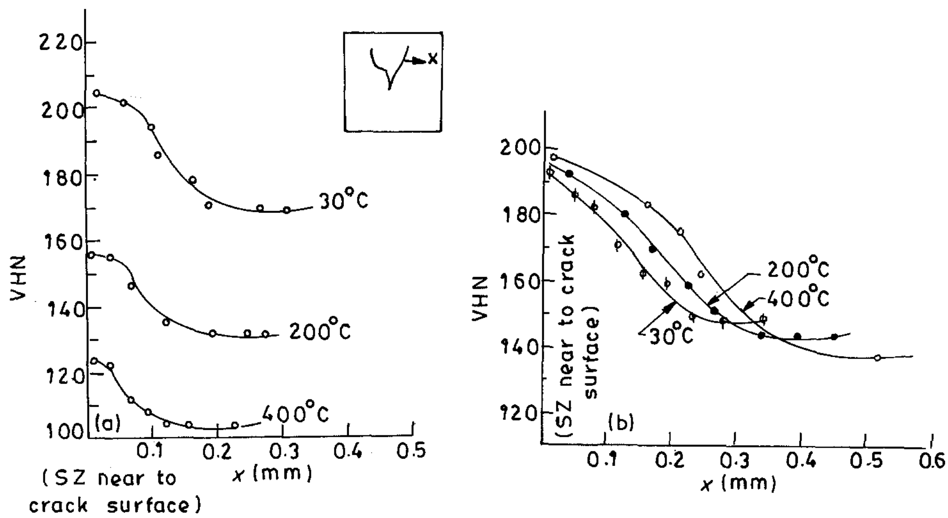

Figure 4 Microhardness distribution in ferrite region (a) Mo steel, (b) Cr–Mo steel.

Mo steel and increase with temperature in Cr–Mo steel. The above trend is similar to the variation of SZW and SZD with temperature in these alloys.

The results on microhardness distribution in ferritic region are shown in Fig. 4. The maximum hardness value was noted at the crack surface which decreased to the minimum (base) level near the undeformed grains. The degree of straining (i.e. maximum hardness–minimum hardness) is found to decrease with increasing temperature in Mo steel and increase with temperature in the Cr–Mo steel (Table III).

4. Discussion

4.1. Different types of crack initiation toughness

The crack initiation toughness, δ_i may be determined in the following four ways.

(i) As the y intercept of the δ–R curve to give CTOD at zero crack growth.

(ii) Intersection of blunting line with R curve. The equation of blunting line may be expressed as,

$$\delta = 2\Delta a \qquad (2)$$

which is deduced from [8].

(iii) CTOD at the intersection of 0.2 mm physical crack growth with R curve as suggested in [9].

(iv) CTOD at the intersection of (critical) SZW on the R curve.

The above approaches to evaluate δ_i are shown in Fig. 5. The δ_i values are presented in Table IV. The δ^0, δ^B, $\delta^{0.2}$ and δ^s represent the δ_i values at zero crack growth, blunting line intersection, 0.2 mm crack growth and SZW intersection, respectively. The subscripts 'av', and max' indicate the δ_i values based on δ_{av} against Δa_{av} and the δ_{max} against Δa_{max} R curves, respectively.

In Cr–Mo steel, the initiation toughness values based on δ_{max} against Δa_{max} R curves are found to be smaller as compared to the toughness values based on δ_{av} against Δa_{av} R curves. At the mid-thickness section, the stable cracking is initiated earlier and its propagation is faster. A small element at the midsection is

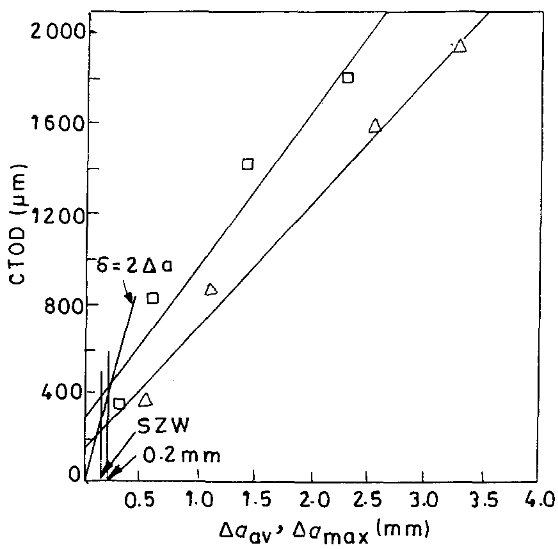

Figure 5 Typical diagram showing δ_i evaluation (Cr–Mo steel, 200 °C) (□ δ_{av} – Δa_{av}, △ δ_{max}—Δa_{max}).

believed to nearly satisfy a plane strain condition and a resistance curve based on the mid-section crack growth (i.e. δ_{max} against Δa_{max} R curve) represents a conservative and realistic situation. In Mo steel, however, the δ_i values based on the δ_{max} against Δa_{max} R curves are not always conservative as compared to the δ_{av} against Δa_{av} R curves. The nature of the R curve in the Mo steel is non-linear, i.e. obtained by employing a second-order polynomial regression whereas the R curve is of a linear nature in the Cr–Mo steel. This is apparently the reason for a difference in the behaviour of δ_i for the Mo steel.

Except for a few cases, the δ^0 values are quite conservative as compared to δ^B, $\delta^{0.2}$ and δ^s values. δ^0 may thus provide a lower limit of initiation toughness and, therefore, may not be a true representative of the actual crack growth resistance of material. Amongst δ^B, $\delta^{0.2}$ and δ^s, the $\delta^{0.2}$ generally appear to provide a crack initiation toughness on the high side leading to an overestimation of δ_i values. The δ^B and δ^s values are fairly comparable.

TABLE IV Crack initiation toughness values in alloys (in μm)

Alloy	Test temperature (°C)	δ^0		δ^B		$\delta^{0.2}$		δ^s	
		δ^0_{av}	δ^0_{max}	δ^B_{av}	δ^B_{max}	$\delta^{0.2}_{av}$	$\delta^{0.2}_{max}$	δ^s_{av}	δ^s_{max}
Mo steel	30	289	318	318	318	325	320	320	320
	200	228	249	235	249	240	249	228	249
	400	82	96	120	110	170	145	125	120
Cr–Mo steel	30	157	75	270	110	325	191	249	140
	200	285	151	440	210	424	262	382	228
	400	237	191	300	220	320	248	307	240

TABLE V A comparison of plane strain initiation toughness

Alloy	Test temperature (°C)	δ_e (μm)	δ_{Ic} (δ_e + 2SZD) (μm)	δ^s_{max} (μm)	δ^B_{max} (μm)
Mo steel	30	25	299	320	318
	200	26	256	249	249
	400	29	139	120	110
HAZ	30	34	276	280	295
Cr–Mo steel	30	31	147	140	110
	200	33	230	228	210
	400	44	266	240	220
HAZ	30	21	159	140	135

4.2. Stretched zone method for CTOD toughness

From Table III it can be seen that the SZD values are invariably smaller than the corresponding SZW values. It is our contention that 2 SZD (at crack initiation) is a more appropriate measure of crack initiation CTOD. It does not, however, include the elastic component of CTOD. The actual crack initiation CTOD would, therefore, be given by

$$\delta_c(\delta_{Ic}) = 2\text{SZD} + \delta_e \quad (3)$$

where δ_e is the elastic component of CTOD. The value of δ_c was obtained by employing experimental SZD values and computing δ_e using

$$\delta_e = \frac{K_I^2(1 - \nu^2)}{2E\sigma_y} \quad (4)$$

The δ_c values thus obtained are given in Table V. As the SZD values used in Equation 3 are based on the mid-thickness measurement, the δ_c values correspond to a plane strain condition and are thus the δ_{Ic} values in reality.

The δ_{Ic} values, as determined above, may be compared with the various initiation toughness values reported in Table V. It is more appropriate to compare the δ_{Ic} values with the initiation toughness determined using δ_{max} against Δa_{max} R curves as these are believed to provide a plane strain condition. Table V shows δ^B_{max} and δ^s_{max} values also along with the δ_{Ic} for the two alloys. A comparison reveals that the δ_{Ic} has better agreement with δ^s_{max} than that of δ^B_{max}. In Mo steel, the δ^B_{max} and δ^s_{max} values are comparable and in fair agreement with δ_{Ic}. For Cr–Mo steel, however, the δ^B_{max} are on the low side whereas the δ^s_{max} have a good agreement. In overall comparison, thus, the δ^s_{max} appears to better represent the crack initiation toughness for plane strain condition amongst the various δ_i values. The initiation toughness δ^s_{max} does not involve any assumptions defining a blunting line unlike δ^B_{max}.

From Tables III and V, a close similarity is noted in the trend of variation of SZW, SZD, 'deformed region length', d, and the δ^s_{max} with temperature in both the steels. This is because the SZW and d are presumably a measure of crack tip ductility which varies with temperature and material. As the strain preceding crack initiation increases, more crack tip opening is required for crack initiation resulting in a higher value of initiation toughness, δ^s_{max}. Simultaneously, an increased amount of stretching at the crack tip also results in enhanced grain deformation. An increase in the hardness of ferrite grains is caused due to enhanced deformation. A close similarity between the degree of straining (hardening) (Table III) and the δ^s_{max} at each temperature further supports a closer link between the grain deformation during stretching and the initiation toughness.

4.3. EGF method for CTOD toughness

The European Group on Fracture (EGF) has proposed a method for determining CTOD for crack initiation [10]. The δ–R curve is obtained in this approach by fitting an equation of the form

$$\delta = A(\Delta a + D)^c \quad (5)$$

where A, D and c are constants to be evaluated. A blunting line equation used in this method is

$$\Delta a = 0.4 d_n G_{eff}/\sigma_0 \quad (6)$$

where G_{eff} is the plasticity corrected strain energy release rate, σ_0 the flow stress and d_n the factor used to account for strain hardening.

An attempt has been made to determine the CTOD initiation toughness using the above method and compare them with the values presented earlier.

The d_n in Equation 6 was taken from Shih's work [12]. The σ_0 in Equation 6 was taken as

$$\sigma_0 = (\sigma_y + \sigma_{tu})/2 \quad (7)$$

where σ_{tu} is the true ultimate tensile stress. Table VI demonstrates the equations for the δ against R curves based on Equation 5 for the two steels. In the other

TABLE VI Equations for δ–R curves and initiation toughness using EGF's method

Alloy	Test temperature (°C)	δ_{av} against Δa_{av} (μm) (mm)	δ_{max} against Δa_{max} (μm) (mm)	$\delta_{av.}^{EGF}$ (μm)	$\delta_{av.}^{EGF}$ (μm)
		$\delta_{av} =$	$\delta_{max} =$		
Mo steel	30	$4.21(\Delta a + 3.99)^{3.0}$		293	—
	400	$435.6(\Delta a - 0.15)^{0.9}$	$120(\Delta a + 0.94)^{0.58}$	124	128
Cr–Mo steel	200	$1325(\Delta a - 0.273)^{0.436}$	$1035(\Delta a - 0.383)^{0.58}$	—	—
	400	$391(\Delta a - 0.63)^{1.04}$	$488(\Delta a - 0.036)^{0.678}$	307	125

For other test situations the curve fitting was not successful

TABLE VII The M values in the J–CTOD relationship

Alloy	Test temperature (°C)	n	m_b	m^a
Mo steel	30	0.190	1.64	1.72
	200	0.212	1.47	1.60
	400	0.203	1.57	1.60
Cr–Mo steel	30	0.170	2.02	1.72
	200	0.203	1.91	1.32
	400	0.186	2.12	2.01

[a] m obtained at $0.06(W - a) \simeq 0.6$ mm

situations, the curve fitting was unsuccessful, i.e. without convergence to give regression coefficients. The initiation toughness values, δ_{av}^{EGF} and δ_{max}^{EGF} using this method are reported in Table VI based on the δ_{av} against Δa_{av} and the δ_{max} against Δa_{max} R curves, respectively. A comparison with Table IV shows that the δ_i values are in good agreement except for the Cr–Mo steel at 400 °C where the difference is considerable.

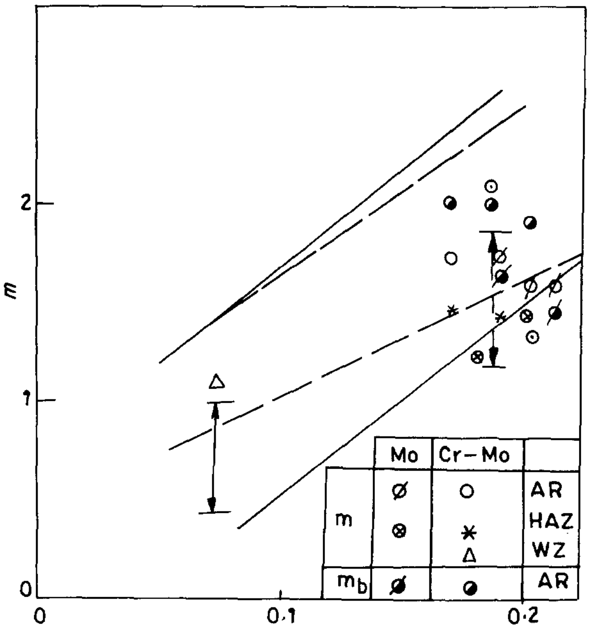

Figure 6 Variation of $m(m_b)$ with n. (∅ Mo, m, AR; ○ Cr–Mo, m, AR; ⊗ Mo, m, HAZ; * Cr–Mo, m, HAZ; △ Cr–Mo, m, WZ; ∅ Mo, M_b, AR; ◑ Cr–Mo, m_b, AR) (‡ Pandey [13], – – – Robinson [14], —— Slatcher [15]).

4.4. J–CTOD relationship

The J integral values were also obtained in the alloys investigated using the standard method [8] as reported elsewhere [11]. The J–CTOD relationship is written as

$$J = m\delta\sigma_0 \qquad (8)$$

where m is a constant. The values of m were obtained during blunting (designated as m_b) and also during crack growth upto $0.06(W - a) \simeq 0.6$ mm. The m_b and m values are given in Table VII. The m_b values are found to vary between 1.47 and 2.12 whereas the m values lie between 1.32 and 2.01 for the alloys investigated.

An attempt has been made to correlate m with the strain hardening exponent, n of the alloys as shown in Fig. 6. The figure also includes data from HAZ and weld zone of alloys taken from [11]. Superimposed on the figure are the results from other investigators [13–15]. Though, most of the experimental points from the present work fall within the scatterband suggested by literature, no clear trend between $m(m_b)$ against n can be inferred. It has been reported [15] that m increases with n upto a limiting value of n beyond which the m remains constant. Nevertheless, it requires further investigation.

5. Conclusions

The conclusions are as follows

1. The crack initiation toughness at 0.2 mm crack growth $\delta^{0.2}$ is higher than the δ^s and δ^B initiation toughness which are based on the stretched zone width and the blunting line ($\delta = 2\Delta a$) approach, respectively.
2. An initiation toughness based on stretched zone depth (δ_{Ic}) has good agreement with δ_{max}^s in both the steels.
3. The crack-tip stretching is followed by elongation and hardening of ferrite grains. The length of deformed grain region (d) and degree of hardening at different temperatures have a trend similar as the initiation toughness, δ^s or δ_{Ic}.
4. The constant factor, m in the J-CTOD relationship lies between 1.3 and 2.1 and has no definite relationship with strain hardening exponent.
5. The EGF method for toughness determination is not applicable in all the situations.

References

1. British Standard Institution Documents, BS 5762, Methods for COD Testing (1979).

2. T. HOLLESTEIN and J. G. BLUEL, *Int. J. Fract.* **13** (1977) 385.
3. S. A. PARANJPE, PhD Thesis, IIT Bombay (1976).
4. G. GREEN and A. WILLOUGHBY, "Fracture and Fatigue", edited by J. C. Radon (Pergamon, New York, 1980).
5. A. WILLOUGHBY, PhD Thesis, University of London (1979)
6. C. R. PRATAP and R. K. PANDEY, *Engng Fract. Mech.* **19** (1984) 1139.
7. O. KOLEDNIK, *ibid*, **29** (1988) 173.
8. Standard Test Method for J_{Ic}, A Measure of Fracture Toughness, ASTM E813–88 (1988).
9. Draft COD Test Method, American Society for Testing and Materials, Philadelphia (1987).
10. K. H. SCHWALBE, B. K. MEALE and T. INGHAM, Proc. ECF6, "Fracture Control of Engineering Structures" (EMAS, U.K.) (1986) 277.
11. P. SUNDARAM, PhD Thesis, IIT Delhi (1989).
12. C. F. SHIH, *J. Mech. Phys. Solids* **29** (1981) 305.
13. R. K. PANDEY, PhD Thesis, IIT Bombay (1976).
14. J. N. ROBINSON, *Int. J. Fract. Mech.* **12** (1976) 723.
15. S. SLATCHER and J. F. KNOTT, *Mater. Sci. Engng* **82** (1986) 37.

Received 1 November 1990
and accepted 25 March 1991